

LONDON, METEOROLOGICAL OFFICE.

Met.O.15 Internal Report No.11.

A computer program to calculate the properties of light scattered by a cloud of spherical particles. By SLINGO, A. and SCHRECKER, H.M.

London, Met. Off., Met.O.15 Intern. Rep. No.11, 1980, 31cm. Pp.7, 5 pls. 7 Refs.

An unofficial document - not to be quoted in print.

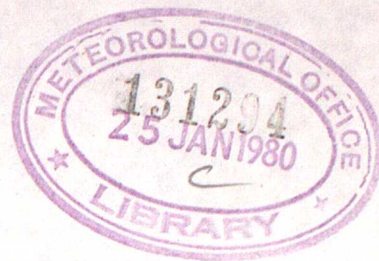
FGZ

National Meteorological Library  
and Archive

Archive copy - reference only



METEOROLOGICAL OFFICE  
London Road, Bracknell, Berks.



# MET.O.15 INTERNAL REPORT

No. 11

A COMPUTER PROGRAM TO CALCULATE THE  
PROPERTIES OF LIGHT SCATTERED BY A  
CLOUD OF SPHERICAL PARTICLES

by

A Slingo and H M Schrecker

January 1980

Cloud Physics Branch (Met.O.15)

FH5B



## 1. INTRODUCTION

This report presents some results from a computer program which calculates the properties of electromagnetic radiation scattered by an ensemble of spherical particles. The single-scattering properties are completely described in the equations first published by G. Mie in 1908, which are therefore commonly referred to as "Mie theory". These equations may be derived by a straightforward, although algebraically lengthy, application of Maxwell's equations with the appropriate spherical boundary conditions. The best book on the subject remains the classic text of van de Hulst (1957). Since the advent of high speed computers, these equations have been the subject of much study and efficient algorithms for solving them have appeared. The heart of our program is a subroutine developed by I.P. Grant and G.E. Hunt at the Atlas Computer Laboratory.

The need for this program has arisen from the work on fog and stratiform clouds in Met O 15. Theoretical and observational studies have shown that the transfer of solar and infrared radiation within clouds makes an important contribution to their energy budget and hence evolution. Comparisons between observed radiative fluxes and those calculated from the Infrared radiation scheme of Roach and Slingo (1979) have shown very good agreement (Slingo, Brown and Wrench, 1980). Similar comparisons are to be made between shortwave fluxes measured using instruments on the MRF C-130 and those calculated by a solar radiation scheme currently being developed. The calculation of shortwave fluxes inside clouds is a much more difficult problem than the calculation of infrared fluxes because of the strong, anisotropic multiple scattering by cloud drops, which occurs at the same wavelengths as absorption by the drops themselves and by water vapour and carbon dioxide. Various mathematical techniques have appeared in recent years to deal with this problem and all require the single-scattering properties of the cloud drops as input data. These are provided by the program described here. The generality of the code is such that it may prove useful in other applications, such as the calculation of the properties of aerosol and haze layers and in the analysis of instruments which use the light scattered from spherical particles to determine their size or composition.



## 2. BASIC EQUATIONS

For a derivation of the equations of Mie theory see van de Hulst (1957). The notation in this report follows that of Deirmendjian (1969).

### 2.1 Basic definitions.

$r$	Radius of particle
$x$	Dimensionless size parameter, $x = kr$ where $k = 2\pi/\lambda$
$m_R, m_I$	Real and imaginary parts of the refractive index of the drops relative to the surroundings.
$\theta$	Scattering angle between scattered and incident radiation.
$Q_{EXT}, Q_{SCAT}, Q_{ABS}$	Efficiency factors for extinction, scattering and absorption. (eg $\sigma_{SCAT} = Q_{SCAT} \pi r^2$ where $\sigma$ is the scattering cross section. For very large particles $Q_{SCAT} \rightarrow 1$ and $\sigma_{SCAT} \rightarrow \pi r^2$ .)
$i_j(\theta) \quad j=1,4$	Dimensionless intensity parameters for Mie scattering.

The Grant/Hunt subroutine provides the efficiency factors and intensity parameters for a single particle at a prescribed set of angles  $\theta$ .

### 2.2 General scattering equations

The single scattering, with no change of frequency, of radiation from a cloud of particles is completely described by

$$\bar{S}(\theta) = \beta_{SCAT} \cdot \frac{\bar{P}(\theta)}{4\pi} \cdot \bar{F}(\theta) \quad \text{--- ①}$$

$$\text{where } \bar{F}(\theta) = \begin{pmatrix} I \\ I_1 \\ I_2 \\ U \\ V \end{pmatrix} \quad \text{and} \quad \bar{S}(\theta) = \begin{pmatrix} I_{s1} \\ I_{s2} \\ U_s \\ V_s \end{pmatrix} \quad \text{are the Stokes vectors}$$

describing the intensity and polarization of the original and scattered light, respectively. Also

$$\bar{P}(\theta) = \begin{pmatrix} P_1(\theta) & 0 & 0 & 0 \\ 0 & P_2(\theta) & 0 & 0 \\ 0 & 0 & P_3(\theta) & P_4(\theta) \\ 0 & 0 & -P_4(\theta) & P_3(\theta) \end{pmatrix} \quad \text{--- ②}$$

is the normalized scattering matrix. The many zeroes in this matrix are due to the spherical symmetry; for particles of arbitrary shape all 16 elements are required.  $\beta_{SCAT}$  is the volume scattering cross section. Similar cross sections for extinction  $\beta_{EXT}$  and absorption  $\beta_{ABS}$  may be defined and are related by



$$\beta_{EXT} = \beta_{SCAT} + \beta_{ABS} \quad \text{--- (3)}$$

The attenuation of a collimated beam through the medium is given by

$$I = I_0 \exp \left\{ - \int \beta_{EXT} dl \right\} \quad \text{--- (4)}$$

So that  $\int \beta_{EXT} dl$  is simply the optical depth,  $\tau$ .

### 2.3 Extension to a distribution of particle sizes

Let the size distribution function of the particles be  $n(r)$  such that  $\int_0^\infty n(r) dr = N$ , the total number of particles per unit volume. If this function is re-defined in terms of size parameter  $x$  then ;

$$\int_0^\infty n(x) dx = k \int_0^\infty n(r) dr \quad \text{--- (5)}$$

It is then possible to define the parameters required by equation 1 ;

$$\beta_{SCAT} = \frac{\pi}{k^3} \int_0^\infty x^2 n(x) Q_{SCAT}(x) dx \quad \text{--- (6)}$$

(and similarly for  $\beta_{EXT}$  and  $\beta_{ABS}$ ).

$$P_j(\theta) = \frac{4\pi}{k^3 \beta_{SCAT}} \int_0^\infty n(x) c_j(\theta) dx \quad j=1,2 \quad \text{--- (7)}$$

From which the following may also be defined;

$$\text{The single scattering albedo} \quad \tilde{\omega} = \beta_{SCAT} / \beta_{EXT} \quad \text{--- (8)}$$

$$\text{The normalized phase function} \quad p(\theta) = \frac{1}{2} [P_1(\theta) + P_2(\theta)] \quad \text{--- (9)}$$

( $p(\theta)$  is normalized so that the integral over all solid angles is  $4\pi$ )

$$\text{The asymmetry factor} \quad g = \frac{1}{4} \int_0^\pi [P_1(\theta) + P_2(\theta)] \cos \theta \sin \theta d\theta \quad \text{--- (10)}$$

The integrals in equations 5 - 10 are approximated in the program by the trapezium rule, using variable resolution in  $dx$  and  $d\theta$ , chosen to maximise accuracy while minimising computing time. The size distribution function  $n(r)$  may be represented in either of two ways. In the first the analytic modified gamma distribution is used (Deirmendjian, 1969) ;

$$n(r) = a r^\alpha \exp(-b r^\gamma) \quad \text{--- (11)}$$

The size distribution is completely defined by specifying the constants  $a, \alpha, b, \gamma$ . In this form the program has been tested against the tabulations of Deirmendjian (1969), giving identical results.

Observed size distribution data may also be read in, as a series of radius values and number densities. Field data obtained with the Knollenberg spectrometer probes, or any such device, can therefore be used directly. Examples will be presented in the following section.



### 3 EXAMPLES

As pointed out earlier, Mie theory provides a complete solution to the single scattering problem with no frequency change, and therefore reproduces all the phenomena predicted by geometrical optics ( $x \gg 1$ ) through to Rayleigh scattering theory ( $x \ll 1$ ). Some of the more familiar phenomena will be illustrated in this section, together with some examples of Cloud Physics applications. To save space, only angular plots of the single function  $p(\theta)$  will be shown.

#### 3.1 Geometrical Optics - the Rainbow

The rainbow is caused by the refraction of sunlight through raindrops, whose diameters are typically 1mm. The size parameter is therefore about  $10^4$ , which is too large for the present program due to the excessive storage and CPU time required. A very narrow size distribution of water drops with average radius  $100\mu\text{m}$  ( $x \sim 10^3$ ) is easily accommodated, however, and still displays all the rainbow features. Figure 1 shows the phase functions for the three wavelengths  $0.40\mu\text{m}$  (Violet),  $0.50\mu\text{m}$  (Green) and  $0.65\mu\text{m}$  (Red). The green and red curves have been displaced downwards by factors of 10 and 100, respectively. Strong peaks are seen at the two rainbow angles, whose positions for raindrops are given by geometrical optics and marked on Figure 1;

$$\text{Scattering angle } \theta = 2\tau - 2p\tau' \quad \text{--- (12)}$$

$$\text{where } \cos \tau = m_R \cos \tau' \quad \text{--- (13)}$$

$$\text{and } \sin^2 \tau = \frac{m^2 - 1}{p^2 - 1} \text{ for } p=2 \text{ (Primary) and } 3 \text{ (Secondary)} \quad \text{--- (14)}$$

The Primary is at the angle of minimum deviation for rays with one internal reflection and the resulting concentration of scattering angles gives the intense bow. The refractive index of water is a function of frequency which displaces the maxima slightly, with Violet towards the anti-solar point ( $\theta = 180^\circ$ ) and Red on the outside of the bow. All rays away from the rainbow angle suffer a larger deviation, resulting in a bright background inside the bow and a dark background on the outside. Interference between two such rays with the same scattering angle produces the "Supernumerary bows", which may often be seen just inside the Primary. These are especially striking in Figure 1 due to the very narrow size distribution used. As the distance from the Primary increases, the supernumeraries merge together to give a white background. The secondary rainbow is at the angle of maximum deviation for rays after two internal reflections. This bow is reversed in every way; the dark region is on the inside so that it reinforces that from the Primary, the colour sequence is reversed



and the supernumerary bows are found on the outside, although these are so faint that they are rarely seen. The most noticeable effect of using  $100\mu\text{m}$ , as opposed to  $1\text{mm}$ , drops in Figure 1 is a displacement and broadening of the rainbow maxima and supernumerary separations as compared to that normally seen.

### 3.2 Cloud Physics applications

As stated in the introduction, this program is to be used to provide single scattering coefficients from water cloud data for a shortwave radiation scheme. Figure 2 illustrates the phase functions at a wavelength of  $0.5\mu\text{m}$  for two size distributions typical of stratiform cloud. The first is the analytic CI distribution used by Deirmendjian (1969) and the second shows data obtained with the Knollenberg ASSP mounted on the M.R.F. C-130 during the JASIN experiment (Data from figure 8 of Kitchen, 1979). Each has been normalized to a liquid water content of  $0.4\text{ g m}^{-3}$ . The larger drops and narrow size distribution of the JASIN data produce a phase function with more detail than the CI distribution, although comparison with Figure 1 illustrates the smoothness in both curves resulting from the much smaller size parameter ( $x \sim 10^2$ ). Both phase functions exhibit the brilliant Aureole within a few degrees of the forward direction, caused by diffraction around the edges of the drops. The aureole is followed by a slow decline through a region whose intensity is virtually independent of size distribution, an effect which is utilised by some types of particle counter. Intensity maxima are seen near the rainbow angles, but these are relatively smooth and broad. Such cloudbows are rarely coloured and are usually seen as a white bow or simply as a change in contrast (Livingston 1979). In the immediate vicinity of the backscatter direction are the highly detailed coloured rings of the Glory. This is sometimes seen by mountaineers when the sun projects their shadow onto mist or cloud below them, and as such is often known as the Brocken Spectre. An excellent example will be seen on the cover of the May 1979 issue of Weather. The complete explanation of the Glory is extremely complex. It is believed to be the result of interference between internally reflected rays of different polarizations, which have "skipped" part of the circumference of the drop as surface waves.

Note the strong dependence of the extinction coefficient on the size distribution. For drops much larger than the wavelength it is easy to show that;



$$\beta_{\text{EXT}} \approx \frac{1500 \cdot \text{LWC}}{\bar{r}} \quad \text{km}^{-1}$$

— (15)

where the liquid water content is in  $\text{g m}^{-3}$  and the mean radius is in microns. For the JASIN data this gives  $60 \text{ km}^{-1}$ , which is in good agreement with the exact result, but for the smaller drops of the C1 distribution the value of  $150 \text{ km}^{-1}$  is too high. The asymmetry factor is only weakly dependent on the size distribution and a value of 0.85 is usually a good approximation in the shortwave region.

Figure 3 shows the phase function for the JASIN data at the infrared window wavelength of  $10 \mu\text{m}$ . The size parameter is now only about 6 and together with the increased absorption the result is a smooth function which, however, is still strongly peaked in the forward direction. As the wavelength is increased still further the asymmetry is gradually reduced. At a wavelength of 8 cm. (Figure 4) the size parameter is about  $10^{-3}$  and the phase function is close to that given by Rayleigh theory,

$$p(\theta) = \frac{3}{4} (1 + \cos^2 \theta)$$

— (16)

The very low extinction coefficient demonstrates the fact that clouds are virtually transparent to microwaves, so that for example they only appear on radar displays if precipitation or ice is present. Rayleigh scattering theory applies whenever  $x \ll 1$ , which is why it also accounts for the blue colouration imparted to the sky by scattering of sunlight from air molecules (for which  $x \sim 10^{-2}$ ).

### 3.3 Other uses

As a final example, Figure 5 shows three phase functions for the analytic Haze M distribution at a wavelength of  $0.589 \mu\text{m}$  (Deirmendjian, 1969). The mode radius is  $0.1 \mu\text{m}$ , giving a size parameter of about unity. The three curves are for different values of the imaginary refractive index and show that an increase in  $m_I$  suppresses the backscatter intensity and thus increases the asymmetry factor. This strong dependence has been used to work backwards from measured phase functions to estimate the value of  $m_I$  for windblown dust particles in the boundary layer (eg Grams et al 1974).

---



REFERENCES

- |   |      |  |
|---|------|--|
| DEIRMENDJIAN D  | 1969 | "Electromagnetic scattering on spherical polydispersions". Elsevier, New York.   |
| GRAMS G W , BLIFFORD I H,<br>GILLETTE D A & RUSSELL P B<br>VAN DE HULST | 1974 | "Complex index of refraction of airborne soil particles". J.App.Met. <u>13</u> , 459-471.  |
| KITCHEN M   | 1957 | "Light scattering by small particles" John Wiley, New York.  |
| LIVINGSTON W C  | 1979 | "A comparison of measuements of cloud liquid water content in stratocumulus between a Knollenberg Axial Scattering Spectrometer Probe and a Johnson—Williams Hot Wire instrument".MRCP 467 |
| ROACH W T & SLINGO A  | 1979 | "The cloud contrast bow as seen from high flying aircraft". Weather <u>34</u> , 16- 17.  |
| SLINCO A, BROWN R & WRENCH C L  | 1979 | "A high resolution infrared radiative transfer scheme to study the interaction of radiation with cloud".Quart.J.R.Met. Soc. <u>105</u> , 603-614.  |
|   | 1980 | "A field study of nocturnal stratocumulus. III.High resolution radiative and microphysical observations." Submitted to Quart. J.R.Met.Soc.   |



Fig. 1

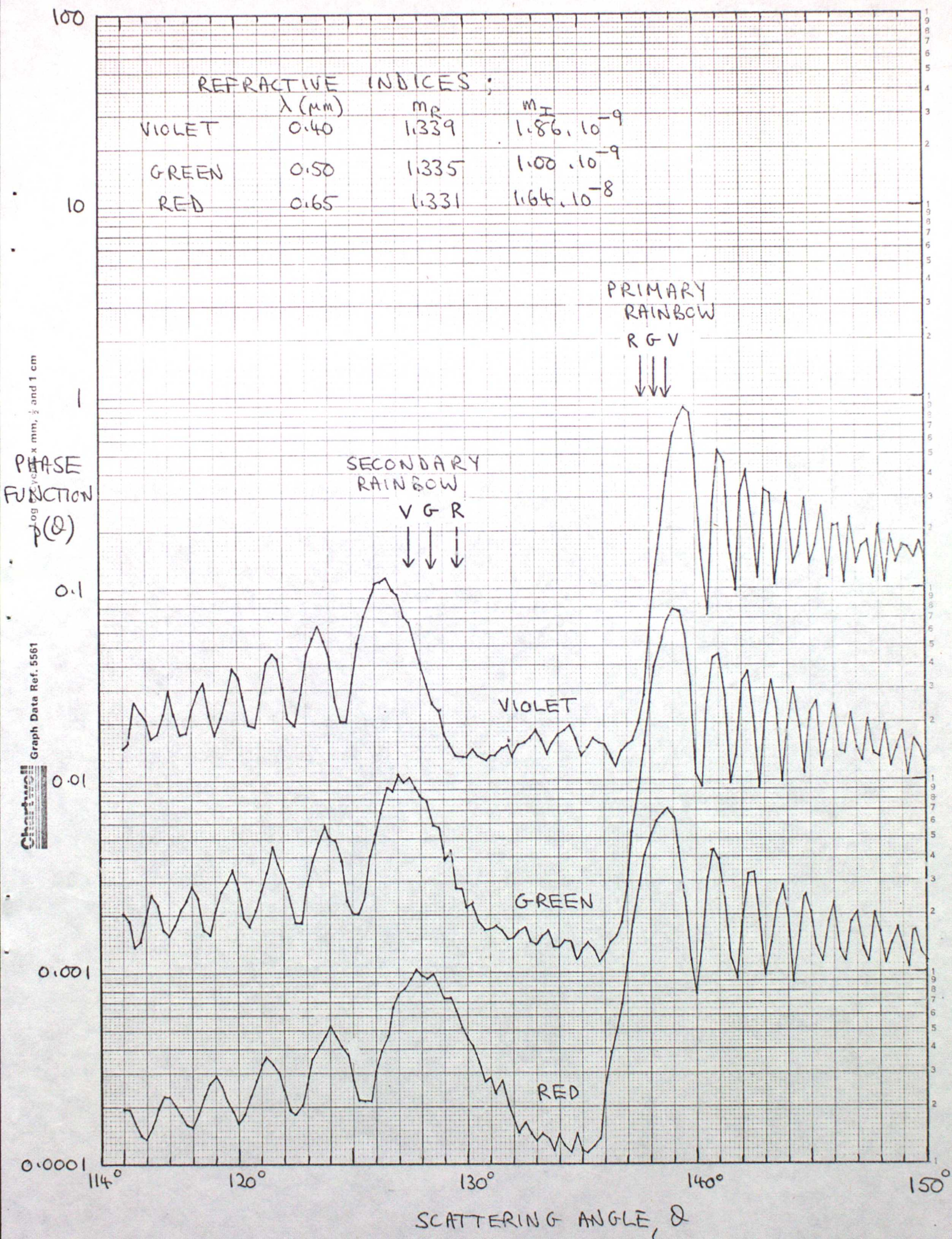




Fig. 2

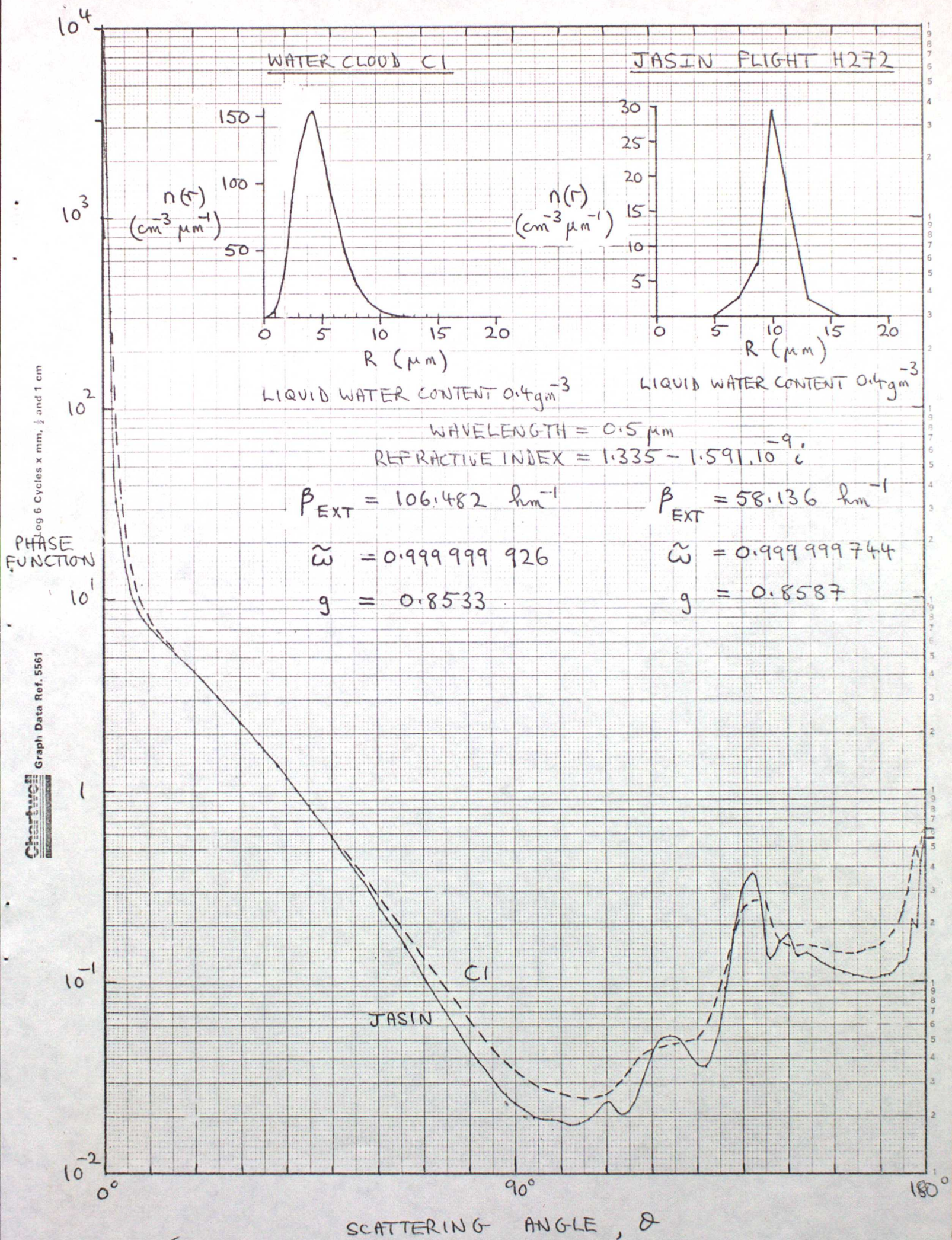




Fig. 3

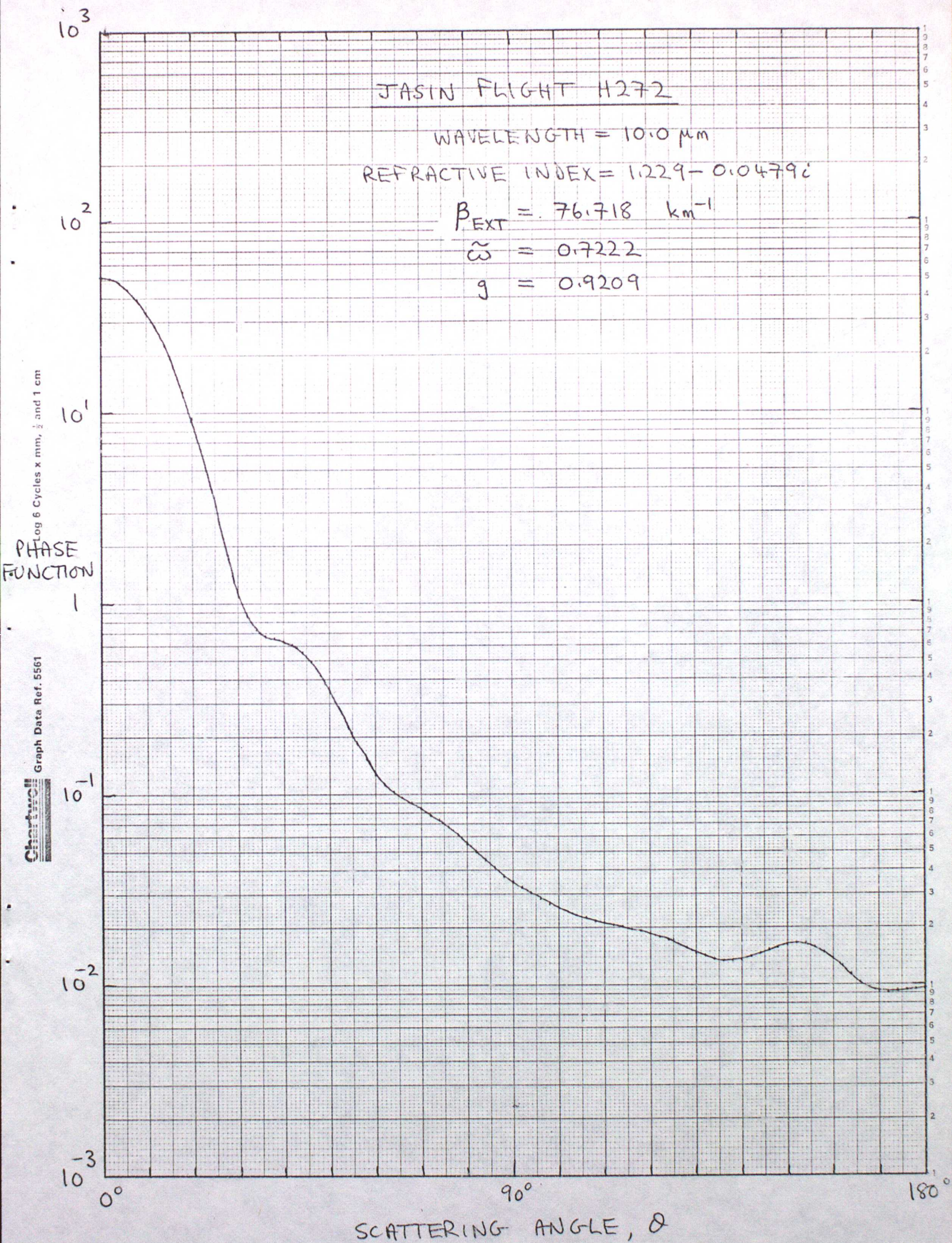




Fig. 4

JASIN FLIGHT H272

WAVELENGTH = 8.0 cm

REFRACTIVE INDEX =  $8.9218 - 1.1423i$

$$\beta_{\text{EXT}} = 8.3984 \cdot 10^{-4} \text{ km}^{-1}$$

$$\tilde{\omega} = 4.66 \cdot 10^{-8}$$

$$g = 2.09 \cdot 10^{-6}$$

log 6 Cycles x mm,  $\frac{1}{2}$  and 1 cm

PHASE  
FUNCTION

Chartwell  
Graph Data Ref. 5561

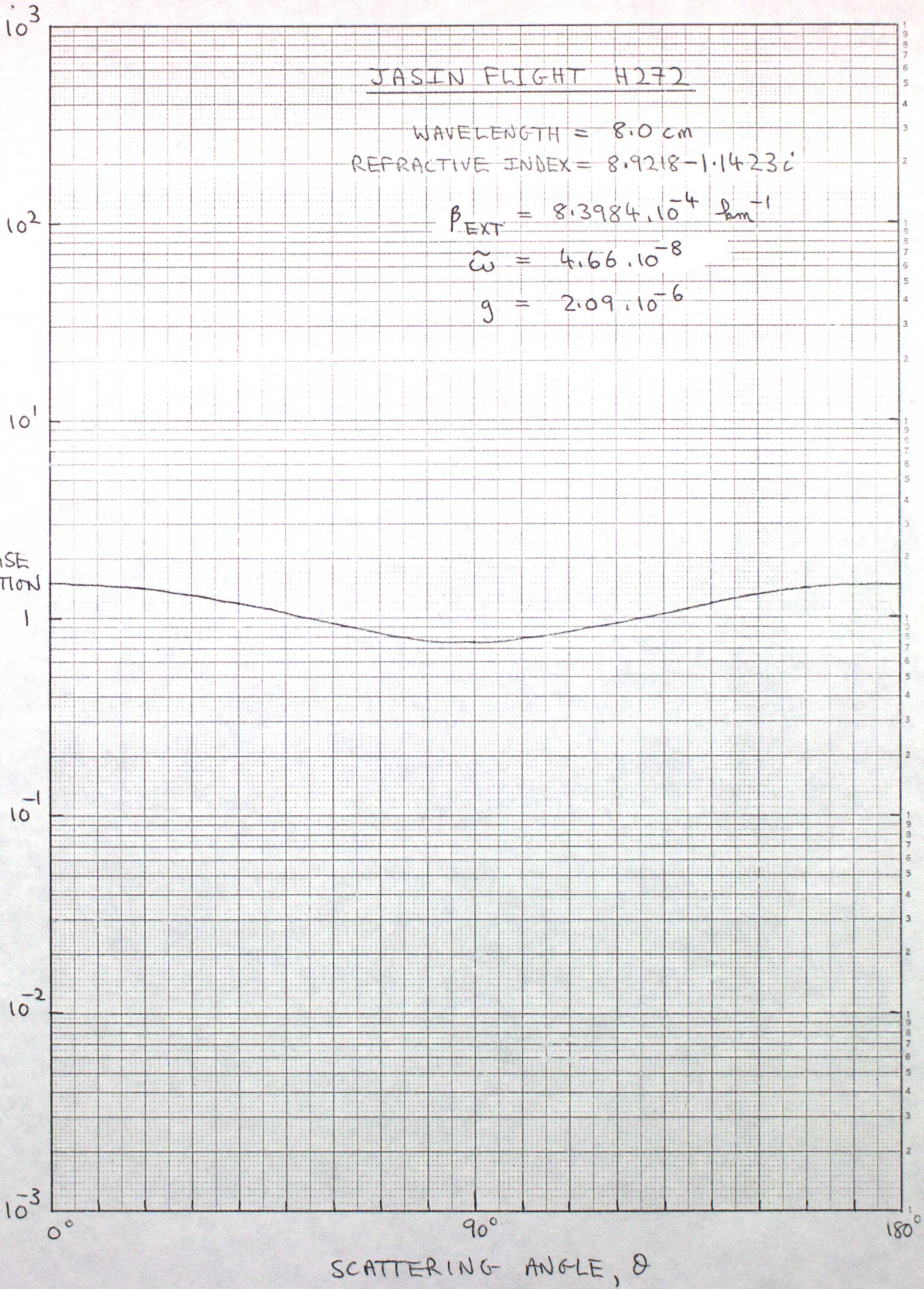




Fig. 5

